The 2020 World Congress on
Advances in Civil, Environmental, & Materials Research (ACEM20)
25-28, August, 2020, GECE, Seoul, Korea

Estimation of combined hardening model parameter values for Korean steel grades

* EunSeon Cho[1)], Jungho Hyun[1)], Sang Whan Han[2)]

[1), 2)] *Department of Architectural Engineering, Hanyang University, Seoul 04763, Korea*

ABSTRACT

To evaluate the structure accurately by using finite element analysis (FEA), a proper material model should be used. For structural members sustaining cyclic loads induced from wind and earthquake loads, a material model that account for should accurately represent the cyclic inelastic behavior of materials. For steel materials, combined hardening models have been commonly used to simulate their inelastic cyclic behavior. The aim of this study is to estimate the combined hardening model parameters for SS275 and SM355 steel, which are commonly used in Korea. Monotonic and cyclic material tests were conducted to obtain low cycle fatigue data. The parameters are determined using the particle swarm optimization (PSO) with test data.

1. INTRODUCTION

Structural materials experience large plastic deformation beyond elastic range when they are exposed to cyclic loadings induced by earthquakes. In current seismic design provisions such as ASCE 7-16 (2016), inelastic behavior is permitted for seismic force resisting systems (Uang, 1991). In order to evaluate the seismic safety of a structure, an appropriate numerical model should be used, by which seismic demands on structural members associated with design earthquake loads could be accurately estimated.

In PEER/ATC 72-1 (ATC, 2010), numerical models to predict inelastic behavior of structural members are classified as lumped plasticity (concentrated hinge) models, distributed inelasticity (fiber) models, detailed continuum finite element (FE) models. Among these three types of models, FE models are the most accurate in predicting local and global behavior of structural members.

However, to obtain reliable analysis results from FE models, the cyclic inelastic behavior of materials should be reflected properly in the FE models (NIST 2017, Mao 2001, Han 2016). Particularly, material models need to reflect low cycle fatigue behavior in plastic ranges under cyclic loading accurately.

[1)] Graduate Student
[2)] Professor

Mild steel exhibits strain hardening behavior beyond yielding when it is subjected to monotonic loading, whereas it shows peculiar behavior under cyclic loading such as Bauschinger effect, cyclic hardening (softening), and ratchetting. Such cyclic behavior is affected by the steel grades (Kaufmann 2001, Versaillot 2017).

The objective of this study was to determine the values of constituent modeling parameters of the combined hardening model. Improved version of opposition-based particle swarm optimization (iOPSO) (Omaran and al-Sharhan 2008) was used to determine the parameter values. Since the parameters of Korean standard steel materials have never been determined, low cycle fatigue tests were conducted for steel grades SS275 and SM355, and modeling parameters for these steel grades were determined using iPSO with test data.

2. MATERIAL TESTS FOR KOREAN GRADES

To investigate the inelastic cyclic behavior of different steel grades and to determine combining hardening parameters of Korean steel grades, this study conducted monotonic tensile tests and low cycle fatigue (LCF) tests with steel grades SS275 and SM355 at room temperature according to ASTM E8/E8M (2016) and ASTM E606/E606M (2012), respectively. Steel grades SS275, SM355 are rolled steels for general structure (KS D 3503 2018) and welded structure (KS D 3515 2018), respectively. The thickness of 16 mm to 40 mm plates were used for coupons. Although monotonic tests were conducted for most steel grades, low cycle fatigue (LCF) tests were rarely conducted due to expensive costs and complexity in experiments. To our best knowledge, LCF tests for these steel grades have never been conducted to estimate their combined hardening parameters.

2.1 Monotonic tensile tests

Monotonic tensile tests were conducted according to ASTM E8/E8M (2016). Standard round shape coupons were made and tested, which had a diameter of 12.5 mm and a gauge length of 50 mm as shown in Fig. 1a and 1b. Loading rates were 0.8 mm/min and 2.5 mm/min before and after yielding point, respectively. Three coupons were made for steel grades SS275 and SM355.

Fig. 1c shows stress-strain curves. The average values of yield (F_y) and tensile strengths (F_u), were estimated as 285 MPa and 428 MPa for SS275, 392 MPa and 505 MPa for SM355, respectively. Table 1 summarizes mechanical properties measured from monotonic tensile tests, where E is the measured elastic modulus, ε_u is the strain at F_u, and ε_f is the strain at fracture. The ε_f value could not be obtained for SS275 because strain gauges fell off from the coupon.

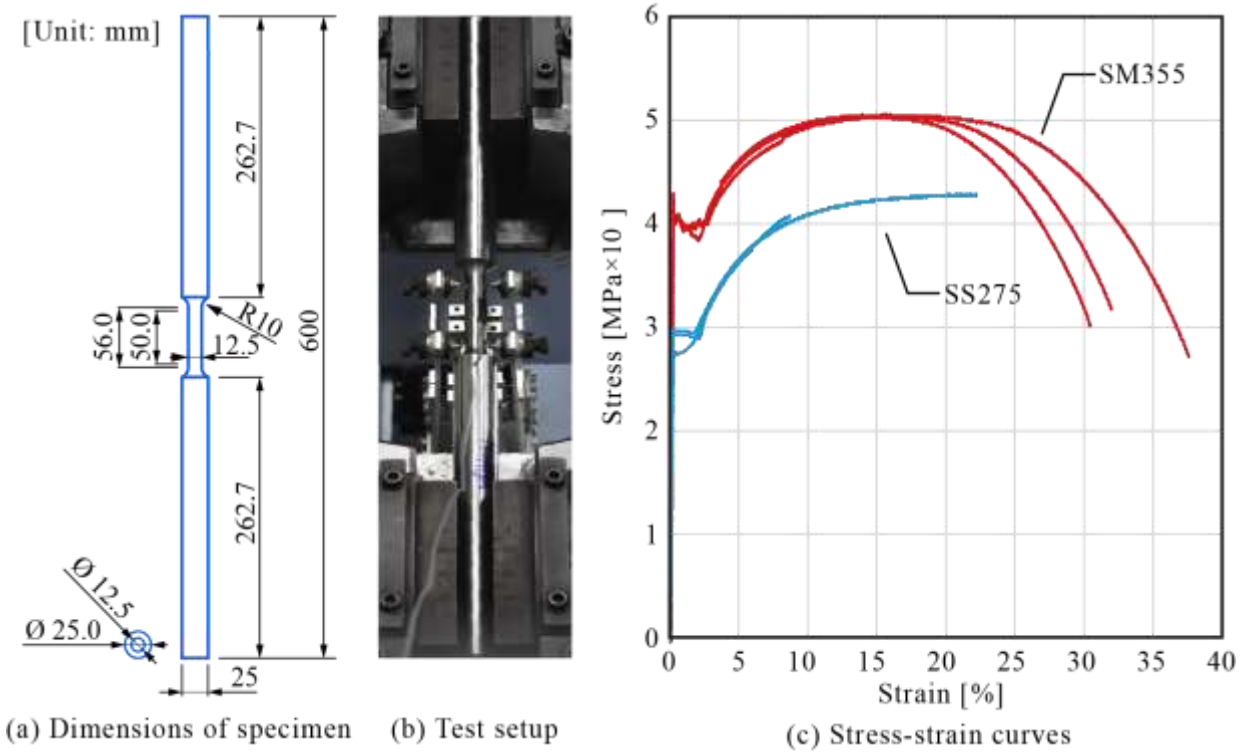

Fig. 1 Monotonic tests

Table 1 Average values of mechanical properties for SS275 and SM355

Specimen	E [MPa]	F_y [MPa]	F_u [MPa]	F_y/F_u	ε_u [%]	ε_f [%]
SS275	212001.7	285	427.9	0.67	21.6	-
SM355	227282.7	391.7	504.5	0.78	15.6	33.3

2.2 Low cycle fatigue tests

Low cycle fatigue (LCF) tests were conducted according to ASTM E606/E606M (ASTM, 2012) with uniform-gauge coupons with a diameter of 10mm and a gauge length of 20mm as shown in Fig. 2a. Fully reversed cyclic loading in tension and compression with a constant strain amplitude ($\Delta\varepsilon$) as shown in Fig. 2b and 2d was used in LCF tests. For mild steels, SS275 and SM355, $\Delta\varepsilon$ of 3%, 4%, 5%, 6%, 7% were used. Thus, for each steel grade, five coupons were made to conduct LCF tests for five different $\Delta\varepsilon$. The loading rate for LCF tests was 0.001 strain/sec (ASTM E606 2012). Fig. 2c shows test setup.

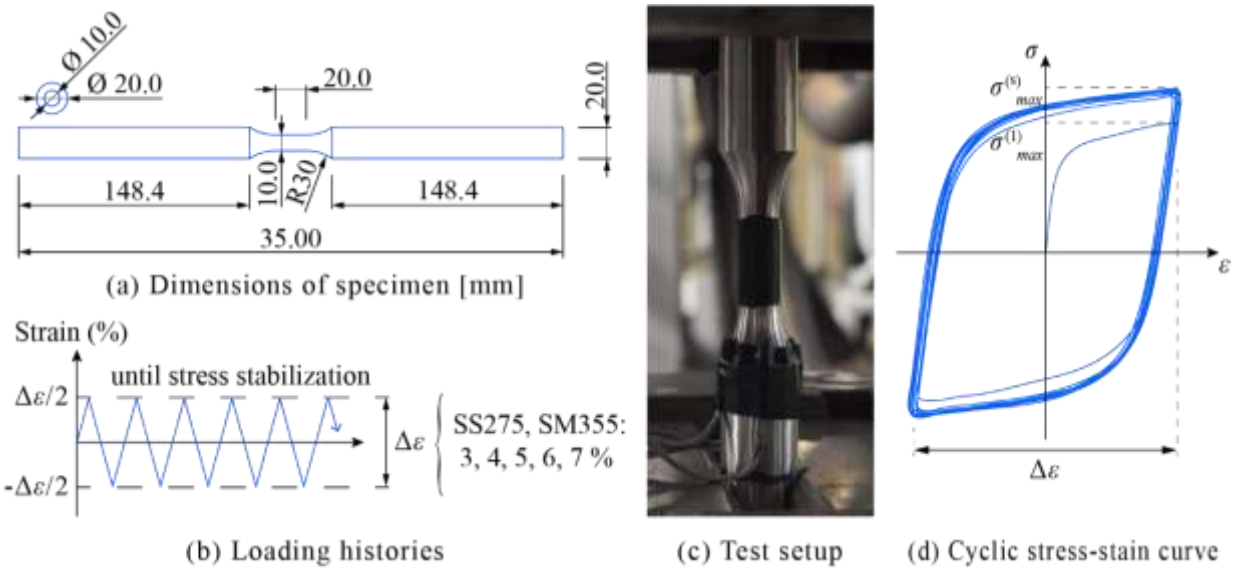

Fig. 2 Low cycle fatigue test with constant $\Delta\boldsymbol{\varepsilon}$

Figure 3 shows cyclic curves obtained from LCF tests. Cyclic strain hardening was observed in SS275 and SM355 steels

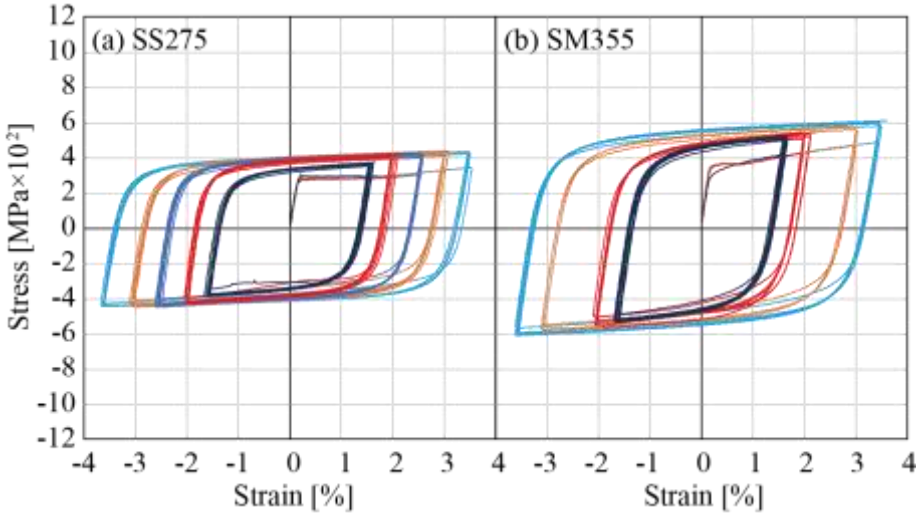

Fig. 3 Cyclic curves obtained from LCF tests

Table 2 summarizes the maximum stress values measured in the first and stabilized cycle ($\sigma_m^{(1)}$, $\sigma_m^{(s)}$), and $\Delta\sigma_m(=\sigma_m^{(s)} - \sigma_m^{(1)})$ for $\Delta\varepsilon$ (Fig. 2d). The $\sigma_m^{(s)}$ values could not be obtained from SM355-C-5 and SM355-C-6 because strain gauge placed on these coupons fell off during the tests.

Table 2 Summary of the LCF test results

Specimen	$\Delta\varepsilon$ [%]	F_y [MPa]	$\sigma_m^{(1)}$ [MPa]	$\sigma_m^{(s)}$ [MPa]	$\Delta\sigma_m$ [MPa]	Hardening behavior
SS275 - C – 3	3	296	297	375	78	Cyclic hardening
SS275 - C - 4	4	282	295	424	129	
SS275 - C - 5	5	277	306	433	127	
SS275 - C – 6	6	285	327	440	113	
SS275 - C – 7	7	294	346	437	91	
SM355 - C – 3	3	339	423	530	107	Cyclic hardening
SM355 - C – 4	4	364	426	549	123	
SM355 - C – 5	5	-	-	-	-	
SM355 - C – 6	6	367	473	-	-	
SM355 - C – 7	7	366	486	613	127	

3. SUMMARY OF COMBINED HARDENING MODEL

The inelastic cyclic behavior of structural steels could not be accurately simulated only with isotropic or kinematic hardening models alone. Isotropic hardening models can describe the cyclic hardening behavior of steel materials but cannot describe the Bauschinger effect inherent in steel materials. In contrast, a kinematic hardening model can simulate the Bauschinger effect but cannot simulate cyclic hardening. In this study, a combined hardening model (Chaboche et al. 1979, 1986), which combines isotropic and kinematic hardening models, was used to simulate the inelastic cyclic behavior of structural steel. This section briefly introduces the combined hardening model.

Initial yield surface can be defined with von-Mises yield criteria Eq. (1).

$$f(\sigma) = J_2(\sigma) - k \tag{1}$$

$$J_2(\sigma) = \sqrt{\frac{3}{2}\sigma' : \sigma'} \tag{2}$$

where f is the yield criteria, k is the initial elastic limiting stress, J_2 is the von-Mises stress, and σ' is the deviatoric stress. When $f < 0$, materials are in elastic range, whereas when $f = 0$, yielding occurs in the materials.

3.1 Isotropic hardening model

The isotropic hardening model expresses inelastic behavior of materials by varying the size of yield surface with fixing the center of surface. These model can be expressed as Eq. (3), which represents an increase in the size of yield surface in plastic range by adding variable R to Eq. (1) according to accumulated plastic strain (p) without changing the center of the surface is illustrated in Fig. 4a.

$$f(\sigma, R) = J_2(\sigma) - k - R \tag{3}$$

$$R = Q(1 - e^{-bp}) \tag{4}$$

where Q and b are the material parameters representing the maximum increase in the yield surface and the rate of the stabilization, respectively. Fig. 4a and 4b show yield surface and stress-strain ($\sigma - \varepsilon_p$) curve with isotropic hardening, respectively. Excursion in cyclic curves with isotropic hardening passes through points 0, 1, 2, 3a, 4a, and 5a when cyclic loading is applied. In the ranges between points 1-2 and 3a-4a, σ is on the yield surface [$f(\sigma, R) = 0$], whereas in the ranges between points 0 and 1, points 2 and 3a, and points 4a and 5a, σ is inside the yield surface($f(\sigma, R) < 0$).Yield surface increases as much as R as shown in Fig. 4a, which accounts for the effect of cyclic hardening. In isotropic hardening models, enlarged yield surface cannot be recovered to initial yield surface (see point 3a in Fig. 4b). Thus, Bauschinger effect cannot be considered only with an isotropic model.

3.2 Kinematic hardening model

Such limitation can be resolved using a kinematic hardening model, in which the size of yield surface does not change, but the center of yield surface migrates by adding backstress (X) as shown in Fig. 4c. Eq. (5) represents the kinematic hardening model.

$$f(\sigma, X) = J_2(\sigma - X) - k \tag{5}$$

$$J_2(\sigma - X) = \sqrt{\frac{3}{2}(\sigma' - X'):(\sigma' - X')} \tag{6}$$

where X' is the deviatoric stress of X.

The backstress, X, is the function of plastic strain (ε_p), in the case of uniaxial loading, which is estimated using Eq. (7) and Eq. (8) for linear and nonlinear model. (Chaboche 1986).

$$X(\varepsilon_p) = \mathrm{C}\varepsilon_p \tag{7}$$

$$X = \nu\frac{C}{\gamma} + (X_0 - \nu\frac{C}{\gamma})e^{-\nu\gamma(\varepsilon_p - \varepsilon_{p0})} \tag{8}$$

where C and γ are material parameters, ν is assigned as 1 for positive loading direction and -1 for negative loading direction, and X_0 and ε_{p0} are the backstress and plastic strain at the beginning of the plastic hardening (points 1, 3b, 5b in Fig. 4b), respectively. Kinematic hardening models can be superposed to simulate plastic behavior more accurately, as in Eq. (9).

$$X = \sum X_i \tag{9}$$

In Fig. 4b, kinematic hardening passes through points 0, 1, 2, 3b, 4b, and 5b. As seen in this figure, kinematic hardening model can account for Bauschinger effect (point 3b in Fig. 4b), but this model cannot represent the growth in yield surface, indicating that cyclic hardening cannot be simulated only using this model.

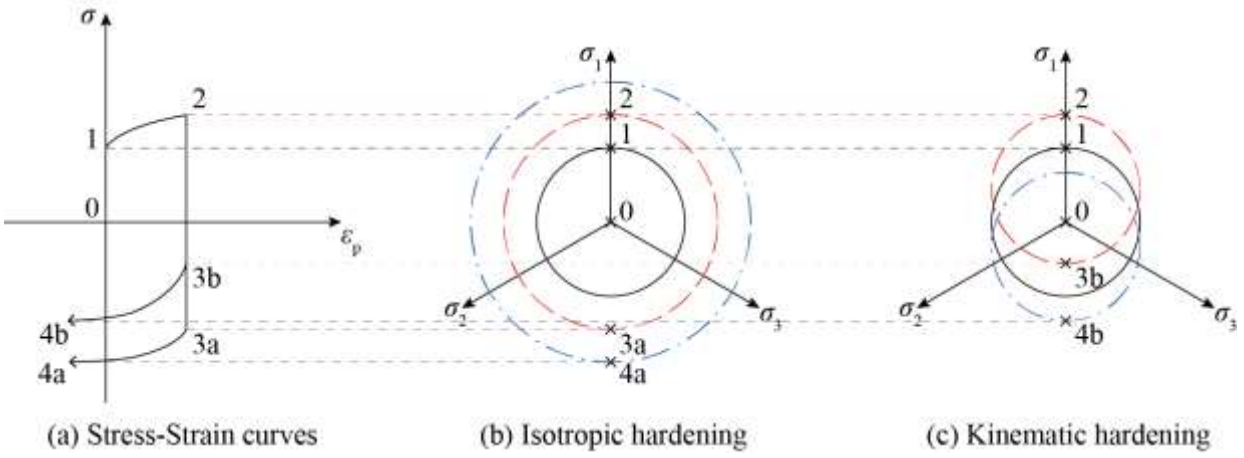

Fig. 4 Schematic representation of isotropic and kinematic hardening model

3.3 Combined hardening model

A combined hardening model Eq. (10) can resolve limitations in isotropic or kinematic hardening models, which is combination of isotropic Eq. (3) and kinematic strain hardening Eq. (5) models. Fig. 5 shows a schematic representation of combined hardening model.

$$f(\sigma, R, X) = J_2(\sigma - X) - k - R \tag{10}$$

$$\sigma\left(k, \varepsilon_p, p\right) = \nu k + \nu R(p) + X(\varepsilon_p) \tag{11}$$

The value of X and R of Eq. (9) enable the movement and size change of the yield surface, respectively, and both the Bauschinger effect and the cyclic hardening can be expressed. For stress in any plastic deformation state, it is expressed as Eq. (10).

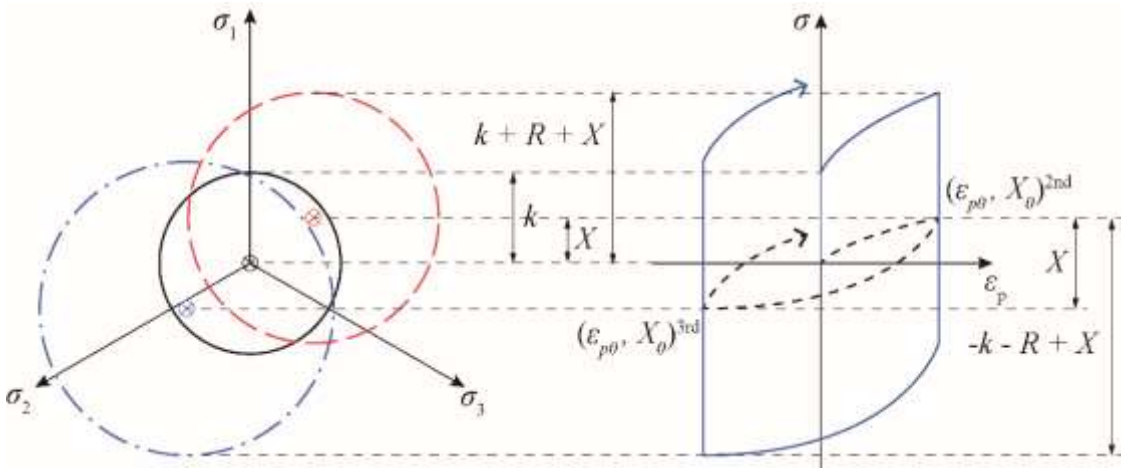

Fig. 5 Combined hardening model

4. DETERMINING COMBINED HARDENING MODEL PARAMETERS OF SS275 AND SM355

In this study, one isotropic hardening and three nonlinear kinematic hardening models were combined to simulate inelastic cyclic behavior of structural steel SS275 and SM355.

Eight model parameters ($Q, b, C_1, \gamma_1, C_2, \gamma_2, C_3, \gamma_3$) for the combined hardening model, and elastic modulus (E) and initial elastic limit (k) should be determined. The PSO was adopted to determine model parameters. The accuracy was verified by comparing measured and simulated LCF curves of Korean structural steel grades SS275 and SM355. The parameters were determined by minimizing an objective function, Ω Eq. (12) using PSO algorithm.

$$\Omega = \mathrm{Min}\left[\frac{1}{M}\sum_{j=1}^{M}\left(\ \frac{1}{N}\sum_{i=1}^{N}\sqrt{(\sigma_i{}^{E}-\sigma_i{}^{A})^2}\ \right)_j\right] \tag{12}$$

where M is the number of specimens for each steel grades, N is the number of data for each specimen, and $\sigma_i{}^{E}$ and $\sigma_i{}^{A}$ are the measured and calculated stresses at the ith step, respectively.

Table 4 summarizes parameter values of and determined from the PSO, and Fig. 6 shows measured and simulated LCF curves at three strain amplitudes.

Table 4 Combined hardening material parameter values of steel grade of SS275 and SM355

	Steel grade	Combined hardening parameter vales from PSO									
		E [MPa]	Q [MPa]	k [MPa]	b [-]	C_1 [MPa]	C_2 [MPa]	C_3 [MPa]	γ_1 [-]	γ_2 [-]	γ_3 [-]
1	SS275	193005	117	138	14.3	78055	5718	956	745	110	4.9
2	SM355	197419	130	170	13.0	169875	35574	5971	1765	475	45.5

5. CONCLUSIONS

In this study, we used combined hardening model that superimposed one isotropic and three nonlinear kinematic hardening models to simulate the nonlinear behaviour of Korea standard steel SS275 and SM355.

There are 8 material parameters ($E, k, Q, b, C_1, \gamma_1, C_2, \gamma_2, C_3, \gamma_3$) values of this model, which is utilized as stochastic optimization algorithms. The optimization algorithm by using Particle Swarm Optimization (PSO) was determined based on the LCF experimental results of each steel.

LCF test was conducted to obtain experimental results. Using the determined material parameter values, the LCF curve was simulated as a combined hardening model, and the resulting curve accurately shows the inelastic cyclic behaviour of each material.

In particular, it was found that the Bauschinger effect due to kinematic hardening and cyclic hardening due to isotropic hardening is well simulated.

ACKNOWLEDGMENTS

It is acknowledged that the research has been supported by grants from the National Research Foundation of Korea (NRF-2020R1A2C2010548). The valuable comment of two anonymous reviewers are also greatly appreciated.

REFERENCES

Applied Technology Council in Cooperation with the Pacific Earthquake Engineering Research Center (PEER/ATC). (2010), PEER/ATC 72-1: “Modeling and acceptance criteria for seismic design and analysis of tall buildings”, PEER/ATC, US.

ASCE 7-16 (2016), Minimum design loads and associated criteria for buildings and other structures, American Society of Civil Engineers, Reston, VA, USA.

ASTM E606/E606M (2012), Standard test method for strain-controlled fatigue testing, American Society for Testing and Materials, West Conshohocken, PA, USA.

ASTM E8/E8M (2016), Standard Test Methods for Tension Testing of Metallic Materials, American Society for Testing and Materials, West Conshohocken, PA, USA

Chaboche, J.L., Dang-Van, K. and Cordier, G. (1979), “Modelization of the strain memory effect on the cyclic hardening of 316 stainless steel”, *Proceedings of the 5th International Conference on SMiRT*, Berlin, Germany, August.

Chaboche, J.L. (1986), “Time-independent constitutive theories for cyclic plasticity”, *Int. J. Plast*, **2**(2),149-188.

Han, S.W., Kim, N.H., and Cho, S.W. (2016), “Prediction of cyclic behavior of WUF-W connections with various weld access hole configurations using nonlinear FEA”, *Int. J. Steel. Struct.,* **16**, 1197-1208.

Kaufmann, E.J., Metrovich, B. and Pense, A.W. (2001), “Characterization of cyclic inelastic strain behavior on properties of A572 Gr. 50 and A913 Gr. 50 rolled sections”, Report No. 01-13, ATLSS, PA, US.

KS D 3503 (2018), Rolled steels for general structure, Korean Agency for Technology and Standards, Seoul, Korea.

KS D 3515 (2018), Rolled steels for welded structures, Korean Agency for Technology and Standards, Seoul, Korea.

KS D 5994 (2018), High-performance rolled steel for building structures, Korean Agency for Technology and Standards, Seoul, Korea.

Mao, C., Ricles, J., Lu, L. and Fisher, J. (2001), “Effect of local details on ductility of welded moment connections”, *J. Struct. Eng.*, ASCE, **127**(9), 1036-1044.

NIST (2017), “Guidelines for nonlinear structural analysis for design of buildings, National institute of standards and technology”, Research Report No.GCR 17-917-46v1, Gathisburgh, MD, USA.

Omran, M.G.H. and Al-Sharhan, S. (2008), “Using opposition-based learning to improve the performance of particle swarm optimization”, *Proceedings of the 2008 IEEE Swarm Intelligence Symposium*, US.

Uang, C. (1991), “Establishing R (or R_w) and C_d factors for building seismic provisions”, *J. Struct. Eng.*, ASCE, **117**(1), 19-28.